The Architecture of a Modular UAV with Additively Manufactured Frame: Preliminary Flight and Performance Evaluations

The Architecture of a Modular UAV with Additively Manufactured Frame: Preliminary Flight and Performance Evaluations

Roberto Torre[1] and Salvatore Brischetto[1]

[1] *Department of Mechanical and Aerospace Engineering, Politecnico di Torino, Torino, Italy*

Abstract: This work explores an Unmanned Aerial Vehicle (UAV) with a customizable configuration. Its architecture follows the application scenario, thus granting it fits the required performances. Tricopter, quadcopter, hexacopter, and octocopter are all the possible configurations this UAV can be adapted to. The customization is achieved with eight individual components; several setups arise when they are assembled in different ways and numbers. The core houses the standard avionics; those to be repeated find place in plug-and-play arms. A further chance of customizability is given by the Fused Filament Fabrication (FFF), the additive manufacturing technology used to produce the structural parts of the frame. Finally, the paper proposes the performance simulation of four different scenarios, implementing non-custom avionics and highlighting how they modify from one setup to another. Flight time, payload capabilities, maximum speed, efficiency, and thrust-to-weight ratio are the key parameters guiding to fit the UAV to the mission profile.

Keywords: UAV; drone; multirotor; additive manufacturing; flight performances.

1. Introduction

Unmanned Aerial Vehicles (UAVs) have a wide field of operation, crossing military purposes, emergency services, photography, and hobbies (Junaid et al., 2018). Multirotors are a specific class of UAVs, drawing attention due to the hovering and vertical take-off; their dimensions, weight, and performances develop over an extended range. This point goes together with the identified application field. The design process of each UAV commonly followed defined (but restricted) performance requirements related to the mission profile. Flight performances result from an accurate propulsion system selection and sizing process but are strongly influenced by several other parameters whose impact is usually difficult to predict in advance.

Corresponding S. Brischetto
Department of Mechanical and Aerospace Engineering, Politecnico di Torino, Torino, Italy
e-mail: salvatore.brischetto@polito.it

T.H. Karakoç et al. (eds.), Name of Symposium Proceedings,
DOI 10.1007/…….

The interdependence of those parameters has many facets: the safety of the UAV increases with the number of propellers, and the same does the load capacity, but this affects the flight time (Mueller et al., 2014); the geometric arrangement of the propellers also defines the flight performances and the controllability in critical conditions (Michieletto et al., 2017). As the payload increases, the inertia follows a similar trend, which leads to a decrease in maneuverability and agility (Mahony et al., 2012); this might prevent applications that require rapid response and robustness to external actions (Rizwan et al., 2019). The design process of the frame requires evaluating the broad spectrum of loads the UAV will undergo during its mission profile (Martinetti et al., 2018). Thus, readily meeting the mission requirements might be difficult; the possibility of iterating the manufacturing and design process up to fitting the project specifications without overcomplicating the design stage is an asset induced by Additive Manufacturing (Zhu et al., 2018).

The design process of any UAV on the market strictly fits the expected application and mission profile. It follows from an optimization phase striving at a fixed purpose. The end-user is then forced to select it from this perspective and switch to other devices when different missions arise. This work discusses a non-limited device, which exploits the Fused Filament Fabrication for its production. Its frame features a modular and adaptive platform; different configurations are possible, each of them modifying its flight performances. Other mission requirements can be accomplished by switching from a design to another.

2. UAV Frame Design

Customization is the key aspect of this design: the UAV benefits from several architectures; at each time, the end-user can choose the most appropriate evaluating the actual application field and the performances it requires. This solution is made possible through a patented geometry. The core has a circular shape and encloses a cylindrical volume designed to house the standard avionics. On the outer surface, it features a rail, to which a set of arms are hooked. Their number ranges from 3 to 8: it is not predetermined as the end-user can select it from a set of specific configurations. The graphical rendering of Figure 1 shows the drone featuring four-arm. The configuration modifies its performances, shaping it to the mission requirements: the end part of the upper and lower surfaces can house a single (S - single, on the upper one) or a pair (D - double, on the upper and lower ones) of motors.

The lower surface can house an inflatable device for shock absorption and water touchdown (A - amphibious) as an alternative to a motor. Once configured, each arm is a plug-and-play device: besides the external equipment, it houses the Electronic Stability Control (ESC). The pattern of the components depends upon the configuration so that the flight control strategy is effective. Several anchor points guide the end-user during the mounting; each features a socket for core-arm connection. The flight control auto-updates once a correct configuration is detected. Manufacturing, upgrading, replacing, and configuring the frame is an easy task: the different parts are eight total. Some elements are always in unit quantity; for others, their number comes from the setup. Their design allows easy production through

Fused Filament Fabrication (FFF) with standard polymers (such as PLA) and home-desktop devices. This work analyzes and discusses a preliminary simulation of the drone performances in four single-motor configurations (S) featuring 3, 4, 6, and 8 arms; those set-ups are labeled as follows: S3A-C, S4A-C, S6A-C, and S8A-C.

Fig.1. Graphical rendering of the UAV in S4A-C.

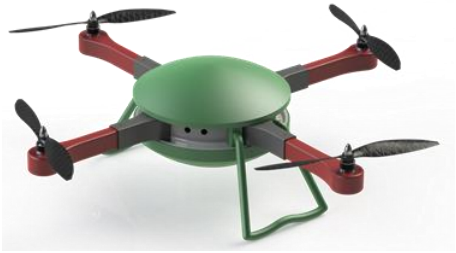

2.1. Components of the frame

The core has been introduced in the previous section. It consists of two circular plates; the upper one features a cylindrical wall enclosing the volume for avionic housing. Ventilation holes are present, together with customizable payload mounts. The external rail allows the arms to be installed and slide to reach the appropriate position, as shown in Figure 2. Each arm is an assembly of three parts with a box shape: an upper and a lower quasi-symmetric components, plus a support that connects them to the core. The profile of this last component allows mounting it on the core. Removable metal fasteners prevent relative sliding between the elements, bind the support to the core, and seal its plates. In addition, anchor points for motor casing are present on the end part of the upper and lower surfaces. The volume enclosed by the elements of the assembly houses the ESC and the arm-specific avionics. The UAV is then supplemented by two spherical domes, shielding any additional electronics and payload and providing additional support to flotation in ditching. As needed, both the domes can be removed or replaced to be transparent and keep the shield function. The drone support on the ground is a prerogative of a couple of landing gears. They fit the external rails of the core; consequently, they are installed together with the arms.

Fig.2. Arm and core assembly in an exploded view.

3. Design and Architecture of the UAV

The chance to modifying the flying configuration has complex implications that go beyond the structure of the frame. Granting modularity without overcomplicating the process left to the final user requires relying upon the same avionics, battery, motors, and electronics in all the set-ups. Therefore, the selection of those components should consider the performances of the different scenarios. The

maximum take-off weight (MTOW) is a place to start; keeping it below 2 kg simplifies the operations from a regulatory perspective (ENAC, 2018). The design process aims to limit the weight of the components, thus leaving sufficient margin to the payload. Such an approach is crucial, as some parts increase their number with that of the arms, increasing their relative influence on the overall weight. The selection of the components and the simulation of the flight performances exploited the simulation suite xcopterCalc (eCalc, 2021): starting from the UAV configuration, the software evaluates and returns its flight performances. It relies on an extensive database of components to be filtered using component-specific parameters. Many parts are interdependent; consequently, the selection process started from those having external constraints. They set further restrictions on the remaining ones, which guided the process.

The frame dimension and weight are the first parameters to be considered for the analysis. The first keeps constant, representing the distance from two opposite engines, which is double the distance between a motor and the center of the UAV. However, the weight of the frame changes with the number of the arms; this leads to four different analyses. The frame design implies coplanar propellers, and their relative distance diminishes as the number of arms increases; this required evaluating the tip clearance for each configuration. It has been chosen to replace them while moving among the setups and selecting the biggest feasible blades per each. As the efficiency of the propellers improves with their dimension, this approach avoided the designs with low arm numbers being negatively affected by the smaller blade dimensions required in higher setups. Then, performance indices have been added to the dimensional requirements to filter the propeller database. The manufacturer usually expresses them with the power constant Pc and the trust constant Tc. The first is to minimize, the second to maximize. The choice fell on Aeronaut CamCarbon propellers, all featuring PC = 0.99 and TC = 1.07. 13" blades for S3A-C and S4A-C, 11" blades for S6A-C, and 8" blades for S8A-C.

Choosing the brushless motors is more complex; xcopterCalc allows a preliminary screening of the models using some parameters as input: the propeller characteristics, all-up weight, the frame size, and the number of rotors, which are all already defined, plus the battery-rated voltage. Next, the tool returns the suggested limits for three datasheet parameters that help select the model: the rpm/voltage, the minimum ESC size, and the minimum motor power. The number of rotors and the propeller characteristics change while moving among the four setups; four screenings have been necessary, which resulted in other ideal ranges.

Table 1: Design ranges for motor selection.

	S3A-C	S4A-C	S6A-C	S8A-C
rpm/V	790 to 1150	680 to 1000	740 to 1080	1090 to 1580
min. power [W]	415 to 725	270 to 475	175 to 305	155 to 275
min ESC [A]	45 to 75	30 to 50	20 to 35	20 to 30

Unfortunately, only a partial overlap between the parameters was detected, which means that an ideal device for all the configurations is tricky to find. The weight is a further important constraint, especially in the designs with a higher number of arms. The analysis leads to select the NeuMotors 1230/5Y. It features a

rpm/voltage of 987, it can provide a maximum continuous power of 250 W and weights only 35 g. ESCs guarantee the connection of each motor with the control unit by controlling its speed; an ESC is needed per arm in S configurations. The previous wizard already provided the minimum ESC size (e.g., the current the ESC can sustain) suggested for each design. However, its dimensions and weight are also vital parameters to consider. A set of intermediate evaluations revealed that the maximum current remains below 18 A in all the designs; this allowed filtering among smaller and lighter devices. The selection process ended with the KISS 18A ESC; it weighs 2 g, and bears a peak amperage of 30 A.

3. Results and Discussion

This section reports the outcomes of the simulations; a set of homogeneous parameters allows comparing the several designs.

Table 2: Weight distribution of the four setups.

	S3A-C	S4A-C	S6A-C	S8A-C
Frame	625 g	684 g	804 g	924 g
Drive	161 g	201 g	280 g	359 g
All-up	1212 g	1311 g	1510 g	1709 g
Payload	788 g	689 g	490 g	291 g

As regards the weight distribution (see Table 2), the outcome is trivial: it increases as more arms are added. This aspect should be considered when heavier payloads are necessary: lower designs should be preferred. The battery-related performances of the UAV reveal nontrivial considerations: the minimum, mixed, and hovering flight times do not follow a monotonous trend. The shorter hovering time belongs to the eight-arm design, confirmed by the lower battery load, indicating a fast discharge. This point should be considered when long-mission are expected. Instead, the first three setups do not show significant differences.

Table 3: Flight times; 6000 mAh, 11V battery at 90%.

	S3A-C	S4A-C	S6A-C	S8A-C
Batt. load	9.68 C	12.6 C	13.2 C	8.44 C
	Flight times [min]			
Min.	5.6	4.3	4.1	6.4
Mixed	14.2	14.0	13.7	12.6
Hover	19.7	20.9	20.6	16.0

The performances of the motors can be evaluated in three different operative scenarios: hovering, maximum, and optimum. The power-to-weight (PTW) ratio at hovering reveals the excellent architecture of the UAV, especially that of the S6A-C: reference values are in the order of 150 W/kg (Sarghini et al., 2017), while more efficient devices drop below 120 W/kg (Qays et al., 2020). The analysis reveals that the absorbed current slightly exceeds the nominal values only in S3A-C, at maximum, but keeps lower than the peak value (30 A); it is significantly lower in all others operative scenarios and configurations. Engine temperatures also feature typical/nominal values; they never exceed 50°C, which is essential given the frame material. The thrust-to-weight (TTW) ratio gives a good measure of maneuverability;

at least a 20% margin of residual thrust at full-throttle is necessary to guarantee the flight (Dai et al., 2019; Half Chrome, 2020). The minimum thrust-to-weight ratio of S8A-C corresponds to 1.8:1; just half throttle is needed to hover the UAV. S6A-C and S4A-C have the highest values, 2.8:1 and 2.7:1, respectively, almost those for racing/acrobatic drones, ensuring great maneuverability; S3A-C lies midway. The last flight performances include the estimated range and the climb rate. The estimated range exceeds 3000 m in all the configurations, reaching almost 4 km in S8A-C; S6A-C, however, stresses the highest climb rate.

Table 4: UAV performance estimation.

	S3A-C	S4A-C	S6A-C	S8A-C
TTW	2.2:1	2.7:1	2.8:1	1.8:1
Est. range [m]	3500	3400	3600	3900
Climb rate [m/s]	5.2	6.0	6.8	5.5
@ hovering				
Current	5.48 A	3.87 A	2.62 A	2.52 A
PTW [W/kg]	151	131	116	131
Temp.	25 °C	22 °C	18 °C	17 °C
@ maximum				
Current	19.4 A	18.9 A	13.2 A	6.33 A
PTW [W/kg]	497	585	533	311
Temp.	50 °C	48 °C	32 °C	20 °C

4. Conclusions

This work demonstrated the possibility of integrating standard avionic components into a customizable and adaptable framework. Furthermore, it validated the potential to maximize or minimize specific parameters to optimize the UAV performance for the intended mission. The choice parameters the end-user can exploit to scroll through the different set-ups are the additional payload, the mission time, and maneuverability. S3A-C: features the highest payload, equal to 788 g, but does not shine for maneuvering performances or flight time. It (slightly) exceeds the standard current managed by the ESC at full throttle. S4A-C: features the maximum hovering flight time plus high thrust-to-weight ratio, although slightly limited in payload compared to the previous. It is a good choice in scenarios requiring high maneuverability but features the minimum estimated range. S6A-C: it slightly improves the thrust-to-weight ratio and estimated range of S4A-C, with similar flight times; it features the best climb rate. S8A-C: it is severely limited in payload, which cannot exceed 291 g to fall within the target category. It features the shortest flight time, 16 minutes, and the lowest thrust-to-weight ratio, 1.8:1, limiting its maneuverability. Its mission range, however, spans almost 4 km.

References

Junaid A. B., A. D. De Cerio Sanchez, J. B. Bosh, N. Vitzilaios and Y. Zweiri, 2018, Design and Implementation of a Dual-Axis Tilting Quadcopter. Robotics 7: 1-20.

Mueller, M. W. and R. D'Andrea, 2014, Stability and control of a quadrocopter despite the complete loss of one, two, or three propellers, IEEE International Conference on Robotics and Automation, May 31-June 7, 2014. Hong Kong, China.

Michieletto G., M. Ryll and A. Franchi, 2017, Control of statically hoverable multi-rotor aerial vehicles and application to rotor-failure robustness for hexarotors, IEEE International Conference on Robotics and Automation, May 29-June 7, 2017. Singapore.

Mahony R., V. Kumar and P. Corke, 2012, Multirotor Aerial Vehicles: Modeling, Estimation, and Control of Quadrotor. IEEE Robotics & Automation Magazine 19: 20-32.

Rizwan R., M. N. Shehzad and M. N. Awais, 2019, Quadcopter-Based Rapid Response First-Aid Unit with Live Video Monitoring. Drones 3: 1-18.

Martinetti A., M. Margaryan and L. van Dongen, 2018, Simulating mechanical stress on a micro Unmanned Aerial Vehicle (UAV) body frame for selecting maintenance actions. Procedia Manufacturing 16: 61--66.

Zhu, W., X. Zhang and D. Li, 2018, Flexible all-plastic aircraft models built by additive manufacturing for transonic wind tunnel tests. Aerospace Science and Technology 84: 237-244.

Ferro, C. G., S. Brischetto, R. Torre and P. Maggiore, 2016, Characterization of ABS specimens produced via the 3D printing technology for drone structural components. Curved and Layered Structures 3: 172-188.

Buhring, J., M. Nuno and K. U. Schroder, 2021, Additive manufactured sandwich structures: Mechanical characterization and usage potential in small aircraft. Aerospace Science and Technology 11: 1-8.

ENAC, 2018, Remotely Piloted Aerial Vehicles Regulation.

https://ecalc.ch, accessed on June 15, 2021.

Sarghini, F. and A. De Vivo, 2017, Analysis of Preliminary Design Requirements of a Heavy Lift Multirotor Drone for Agricultural Use. Chemical Engineering Transactions 58: 625-630.

Qays, H. M., B. A. Jumaa and A. D. Salman, 2020, Design and Implementation of Autonomous Quadcopter using SITL Simulator. Iraqi Journal of Computers, Communications, Control & Systems Engineering 20: 1-16.

Biczyski, M., R. Sehab, J.F. Whidborne, G. Krebs and P. Luk, 2020, Multirotor Sizing Methodology with Flight Time Estimation. Journal of Advanced Transportation: 1-15.

https://www.halfchrome.com/drone-thrust-testing/, accessed on February 2020.